RESEARCH PAPER

Adsorption Study of Pb(II) Ions on the Blast Furnace Slag (BFS) from Aqueous Solution

Toufik Chouchane*, Sana Chibani, Ouahida Khiriddine, Atmen Boukari

* *chouchane_toufik@yahoo.fr & t.chouchane@crti.dz*

Research Center in Industrial Technologies CRTI, P.O. Box 64, Cheraga 16014, Algiers Algeria

Received: September 2022 **Revised: November 2022** **Accepted: January 2023**
DOI: 10.22068/ijmse.3011

Abstract: *In this work, blast furnace slag (BFS) was used as an adsorbent material for the removal of Pb (II) ions in solution in batch mode. The physico-chemical analysis used indicated that the BFS is essentially composed of silica, lime, and alumina. Its specific surface area was 275.8 m^2/g and its PZC was around 3.8. The adsorption study indicated that the maximum amount of Pb (II) adsorbed under optimum conditions (agitation speed (V_{ag}): 150 rpm; pH: 5.4; particle size (Øs): 300µm, T: 20°C) was 34.26 mg/g after 50 minutes of agitation, and adsorption yield was best for feeble initial concentrations. The most appropriate isothermal model was that of Langmuir, and the adsorption speed was better characterized by the pseudo-second order kinetic model. The adsorption mechanism study revealed that internal diffusion is not the only mechanism that controls the adsorption process and there is also an external diffusion, which contributes enormously in the transfer of Pb (II) from solution to adsorbent. Thermodynamic study indicated that the Pb (II) adsorption on the blast furnace slag (BFS) was spontaneous, exothermic, and that the adsorbed Pb (II) is more ordered at the surface of the adsorbent.*

Keywords: *Adsorption, Slag, Pb (II), Kinetics, depollution.*

1. INTRODUCTION

Liquid discharge containing Pb (II) is harmful to humans and their environment due to its harmful effects [1]. In fact, the ions Pb (II) are hardly degradable and have a negative impact on the environment's self-cleaning processes and their bioaccumulations, favoring the toxicity of living organisms [2]. Pb (II) can come from several production activities such as Mining, production of non-ferrous metals, foundry waste, alloys, paints, storage batteries, cable sheaths, products for use in plastics and industries automobiles [3]. Removal of such a harmful element requires treatment of choice, such as chemical precipitation [4], coagulation/flotation [5], membrane technologies [6], ion exchange [7], electrochemical technologies [8] and adsorption phenomenon [9]. Amongst these processes, adsorption is considered to be one of the best processes employed for the removal of metal ions in solution due to its simplicity, high efficiency, and reasonable price [10]. According to the literature, adsorbents used in the Pb (II) removal processes in solution are generally the carbon-based adsorbents [11], clay minerals [12], polymers [13], wood waste [14], nanocomposite [15] and nanomaterials [16]. In this study, blast furnace slag (BFS) has been chosen as a trustworthy, present in large quantities, and less expensive adsorbent. This material is a co-product of the metallurgical steel industry. It is formed during the production of pig iron from iron ores in the blast furnace. In the world, the annual production of BFS is very important. It amounts to tens of millions of tons [17], which represents a real environmental problem and a waste of considerable financial resources [18]. Previous researches have indicated that blast furnace slag is an effective adsorbent in the field of water treatment, especially in the elimination of metal ions, phosphorus, and dyes. Indeed, El-Dars et al. [19] mentioned that water-cooled blast furnace slag showed good potential as an adsorbent to remove divalent nickel ions from aqueous solutions. Scott et al. [20] reported that steel slags have been shown to be an effective means of phosphorus removal and a potential aid in reducing point and non-point source phosphorus pollution in fresh waters. However, Dhmées et al. [21] demonstrated that silica nanoparticles obtained from blast furnace slag and desilicated blast furnace slag can be used as a low-cost adsorbent to remove methylene blue from water.

The principal objective of this study was to introduce blast furnace slag (BFS) in the field of pollution control of waters containing Pb (II). The

[DOI: 10.22068/ijmse.3011]

approach consisted of evaluating the adsorption capacity of BFS to eliminate Pb (II) in solution under different experimental conditions as a first step. The second step is to define the adsorption isotherms, calculate the reaction velocity, identify the mode of Pb (II) diffusion from the solution to the BFS, and investigate the nature of the elimination process. It is obvious that the preparation and characterization of the solid had to be done beforehand. In this work, X-ray diffraction, X-ray fluorescence, and infrared were used for the physico-chemical characterization of BFS. However, its specific surface area (SSA) was measured using the BET method. Otherwise, the agitation speed (V_{ag}), pH, temperature, particle size (Øs) and initial concentration were used to assess the yield of the Pb (II) adsorption on BFS. Langmuir, Freundlich and Temkin models were used for presenting the adsorption isotherms. Kinetic models were utilized to describe the kinetics and mechanisms of the adsorption process. The thermodynamic parameters were investigated to study the energy exchanges. The purpose of this study is to confirm that BFS is a reliable adsorbent that can contribute to the decontamination of water containing metal ions.

2. EXPERIMENTAL PROCEDURE

2.1. Treatment of BFS

The Samples of the BFS were collected at the El-Hadjar steel complex Annaba/Algeria, in the form of rocks with dark color. The washing performed at the crude slag is represented as follows [22]:

- The considered BFS samples were washed with distilled water and air dried for 48 hours.
- The washed samples were grinded and sieved to various size: 200, 300, 400 and 500 µm.
- Samples with different grain sizes were separated, washed with distilled water, steamed at 105°C and stored in plastic boxes for subsequent use in adsorption processes.

2.2. Analytic Methods

Pb (II) concentration was measured by atomic absorption spectroscopy method using PerkinElmer 3110 equipments. The pH of solution was measured with an Ericsson pH metter. The characterization was carried out by X-ray fluorescence (Siemens SRS 3000), X-ray diffraction (Rigaku Ultim IV) and Fourier transform infrared spectrometer (Perkin Elmer).

2.3. Adsorption Protocol

A series of batch experiments were conducted to evaluate the Pb (II) adsorption process on BFS. These experiments will allow us to determine the maximum adsorbed capacity, investigate the adsorbate-adsorbent interaction, define the reaction speed order of the process, determine the method of Pb (II) diffusion from the solution to the BFS surface, and specify the nature of adsorption. Adsorption kinetics were investigated by adding one gram of BFS to aqueous solutions prepared with Pb (II) nitrate ($Pb(NO_3)_2$, $6H_2O$) at a low level. The concentrations prepared vary from 10 to 80 mg/L and the solution volume is 1 liter. The continuous mixing of the solution was ensured during all the tests by mechanical stirrer at different speeds. The temperature was controlled with a water bath equipped with a thermostat. The adsorption kinetics were followed by sampling of 5 ml every 10min. The samples taken were stocked in flasks and the concentration of Pb (II) ions was measured using atomic absorption spectrometry (AAS).

The results of Pb (II) adsorption in this study were analyzed in terms of adsorptive capacity (q), as determined by equation 1:

$$q_t = \frac{C_0 - C_t}{m} \times V \quad (1)$$

Efficiency of Pb (II) adsorption in this study is calculated by the following equation (eq. 2):

$$\%R = \frac{C_0 - C_0}{C_0} \times V \quad (2)$$

Where: C_0: Initial concentration of the metal solution (mg/L); C_t: Concentration of the metal solution after a time t (mg/L); C_e: Concentration of the metal solution after at equilibrium (mg/L); V: Volume of the solution (L); m: Adsorbent mass (g).

The operating conditions undertaken in this study are given as follows:

- Equilibrium time: C_0: 30 mg/L; $V_{ag.}$: 150 rpm; pH: 4.4;T= 20°C; Øs :400 µm; Ms: 1 g.
- Effect of Øs: C_0: 30 mg/L; $V_{ag.}$: 150 rpm; pH: 4.4;T= 20°C; Øs :400 µm; Ms: 0.2, 0.4, 06, 0.8, 1. 1.2, 1.4 g.
- Effect of pH: C_0: 30 mg/L; $V_{ag.}$: 150 rpm; pH=2, 4.4, 5.4 and 6; T: 20°C; Øs :400 µm; Ms: 1 g.
- Effect of T: $C_{0.}$: 30 mg/L; V_{ag}: 150 rpm; pH: 5.4; T: 20, 40 and 50°C; Ø :400 µm; Ms: 1 g.
- Effect of Øs: $C_{0.}$: 30 mg/L; V_{ag}: 150 rpm; pH:

[DOI: 10.22068/ijmse.3011]

5.4; T :20°C; Øs : 200, 300 and 400 µm . Ms: 1 g.

- Effect of C_0: C_0.: 10-80 mg/L; V_{ag}: 150 rpm; pH: 5.4; Øs: 300 µm, T:20°C; Ms: 1 g.

Where: BFS: the blast furnace slag C_0: initial concentration (mg/L); $V_{ag.}$: agitation speed (rpm); Øs: BFS particle size (µm); Ms: BFS mass (g); T: solution temperature (°C).

3. RESULTS AND DISCUSSION

3.1. Characterization of BFS

The BFS from Sider El-Hadjar complex is mainly composed of alkaline oxides CaO, MgO and acidic oxides Al_2O_3, SiO_2. In which the content of CaO is 37.2%, MgO is 3.12%, Al_2O_3 is 8.2%, and SiO_2 is 41.1% (table 1). In addition, BFS has a small amount of other metal oxides (Fe_2O_3, NiO, K_2O, and Na_2O) (table 1).

Table 1. Table1. Chemical composition of BFS [22].

Element	Mass %
CaO	37.2
Al_2O_3	8.2
SiO_2	41.1
Fe_2O_3	2.51
MgO	3.12
MnO	2.64
K_2O	0.3
Na_2O	0.7
LOI	4.23

The tests realized by X-ray diffraction indicated that the BFS is essentially composed of the lime, the silica and the alumina in less quantity (Fig. 1(a)). FT-IR spectrum of fraction shows the stretching vibrations of 1793, 879 and 715 cm^{-1} whose origins are due to the stretching vibration of $COCa_3$ (Fig. 1(b)). The observed peak at 1437cm^{-1} indicated the bond elongation CO. However, the Si-O-Si and Al-O bonds were indicted by the vibrations bands respectively at 1007 cm^{-1}, 634cm^{-1} (Fig. 1(b)). These observations were justified by the results obtained by X-ray fluorescence.

The specific surface areas (SSA) of the BFS particles were obtained by using the nitrogen gas adsorption-desorption method. The Brunauer, Emmett, and Teller (BET) model was used to analyze the isotherm data for nitrogen gas desorption at 77 K. The result of the investigations has shown that the specific surface is 275.8 $m^2.g^{-1}$.

3.2. Adsorption Studies

3.2.1. Effect of agitation time

The contact time required to effectively remove pollutants by the adsorption process is a very considerable variable because it tells us about the equilibrium time and the saturation of the adsorbent.

The kinetic study revealed that Pb (II) adsorption was rapid for the first 30 minutes, then gradually decreased until it was non-existent. Increasing the contact time further yielded no further adsorption for 190 min, which followed (Fig. 2(a)). This means that the adsorbent has reached the saturation phase.

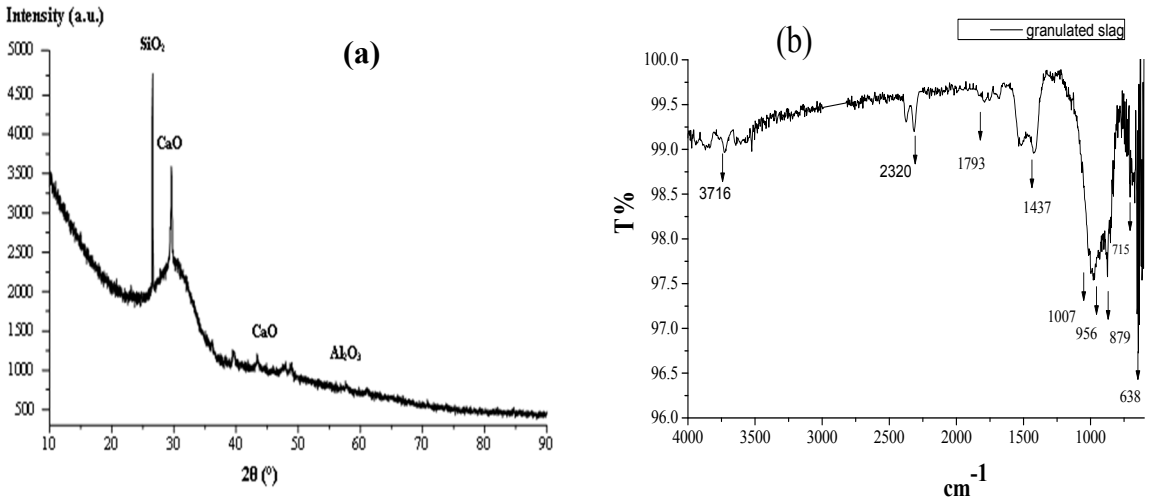

Fig. 1. a) Diffractogram of BFS sample [22], b) infrared spectrum of BFS sample.

[DOI: 10.22068/ijmse.3011]

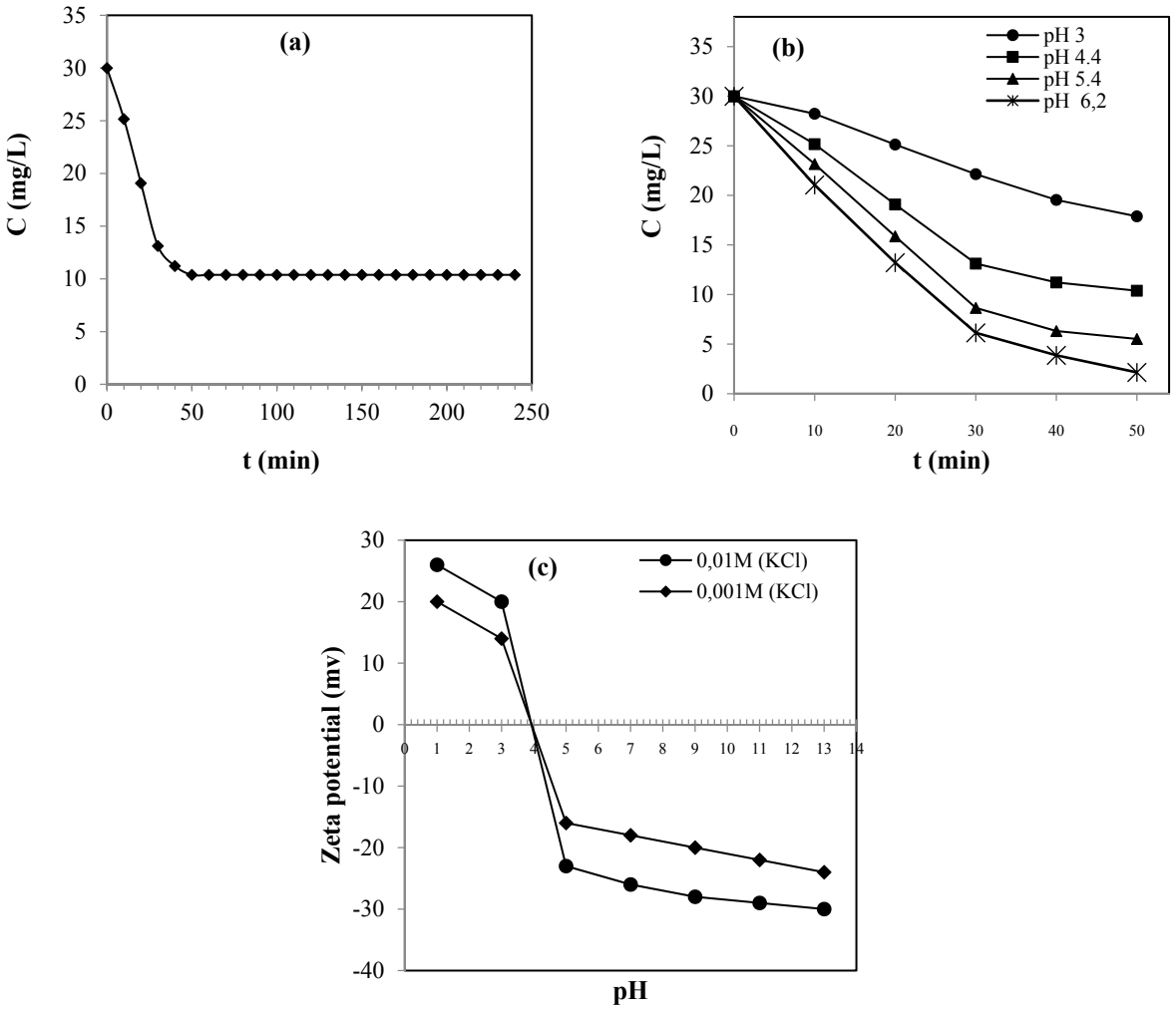

Fig. 2. a) Effect of agitation time, b) Effect of pH, c) Zeta potential as a function of pH.

Indeed, the stopping of the adsorption process is generally generated by the saturation of the surface of the adsorbent, that is to say, the total occupation of the active sites of adsorption by the lead ions. Consequently, we consider 50 min as the equilibrium time of Pb (II) adsorption by BFS.

3.2.2. Effect of initial pH

The pH of the solution is an important parameter in the adsorption phenomenon because it affects the form of metal in solution, as well as the surface properties of the adsorbent [23]. In this work, The effect of pH on Pb (II) adsorption was investigated over a pH range from 3 to 6.2 (3, 4.4, 5.4, and 6.2), at a contact time of 50min (Fig. 2(b)).

At pH 3, the adsorption process was the least efficient (Fig. 2(b)). For this medium, the strong presence of H^+ ions slows down the transfer of Pb (II) ions from the solution to the adsorbent [24]. As initial pH increased from 3 to 5.4, the residual concentration decreased from 17.88 to 5.52 mg/L (Fig. 2(b)). Indeed, the efficiency of adsorption can be explained by the effect that the pH of the solution has favourably influenced the surface charges of adsorbent by turning it negative [25]. Due to this result, we hypothesized that Pb (II) adsorption on blast furnace slag was caused by the electrostatic interaction [22]. Indeed, Fig. 3(a) shows that the pzc of the adsorbent corresponds to pH= 3.8, which indicates that the surface of the blast furnace slag is negatively charged at a pH greater than 3.8.

For an initial pH of 6.2, the quantity eliminated is more important. The concentration at equilibrium and the rate of elimination are, respectively: 2.15 mg/L and 92.83%. This outcome was obtained by the phenomena of adsorption and chemical precipitation. Indeed, the lead ions (Pb^{++}) are

[DOI: 10.22068/ijmse.3011]

precipitated by the hydroxide anion that forms the precipitate of lead hydroxide when the pH approaches 7 [26]. Accordingly, pH= 5.4 value was selected as optimum pH for Pb (II) adsorption. A similar study found that steel slag eliminates the most Pb (II) at pH 5 [27].

3.2.3. Effect of temperature

The solution temperature has important effects on the adsorption process [28]. In this context, the effect of temperature on Pb (II) adsorption was investigated. The temperatures studied are varied from 20 to 50°C (Fig. 3(a)).

The results showed that the Pb (II) adsorption capacity decreased with the increase in temperature (Fig. 3(a)). With increasing temperature, the mobility of Pb (II) ions increased, thereby resulting in the escape of ions from the solid phase to the liquid phase. Therefore, the lead adsorption process on the BFS is becoming less and less favorable [29]. This result led us to predict that the Pb (II) adsorption process on BFS in solution is exothermic [30].

3.2.4. Influence of particles size

The adsorbent granulometry has a predominant role in the rate of transfer of metal ions from the solution to the adsorbent [31]. In this context, we have optimized the particle size of BFS using diameters varying from 200 to 500 µm (Fig. 3(b)). According to the test results, Pb (II) adsorption on BFS is better for particle sizes corresponding to 300 µm. Indeed, the adsorption rate regressed from 91.73% (300 µm) to 66.26% (500 µm) as the particle size increased. The increase in particle size resulted in the narrowing of the BFS adsorption surface area, which caused the regression of the adsorption rate [32]. However, at particle sizes Φs= 200 µm, the Pb (II) adsorption in solution on the BFS was found to be the least favourable (Fig. 3(b)). This result could be clarified, probably by the phenomenon of coalescence [33].

3.2.5. Effect of adsorbent dosage

The study of the impact of the adsorbent mass on the adsorption process is an essential step, since it informs us about the appropriate optimal mass.

From Fig. 4(a), it was observed that the adsorption rate increases with the mass of the adsorbent. This phenomenon can be explained by the increase in free active sites on the adsorbent surface [34]. Furthermore, it was observed that at high adsorbent masses (m >1 g), the adsorption rate regresses slightly. The slight regression observed was probably caused by the agglomeration of slag particles from the blast furnace [35]. Accordingly, 1 g was selected as the optimum mass of adsorbent.

3.2.6. Effect of initial concentration

The initial concentration is a very important parameters in the Pb (II) adsorption process [36]. In this context, we have ranged the concentration from 10 to 80 mg/L (Fig. 4(b)).

The experimental data indicated that the adsorption capacity gradually increases up to a certain value, then it becomes constant (9.32 to 36.24 mg/g) (Fig. 4(b)). After 50 minutes of stirring, the maximum adsorption capacity of Pb (II) in solution on the BFS under optimal experimental conditions is 36.24 mg/g.

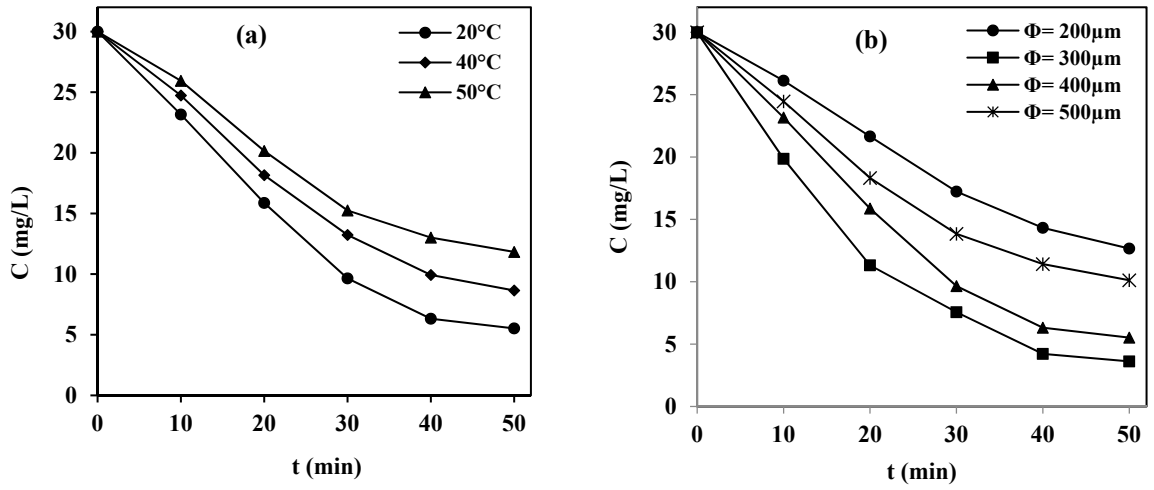

Fig. 3. a) Effect of temperature, b) Effect of particle size.

[DOI: 10.22068/ijmse.3011]

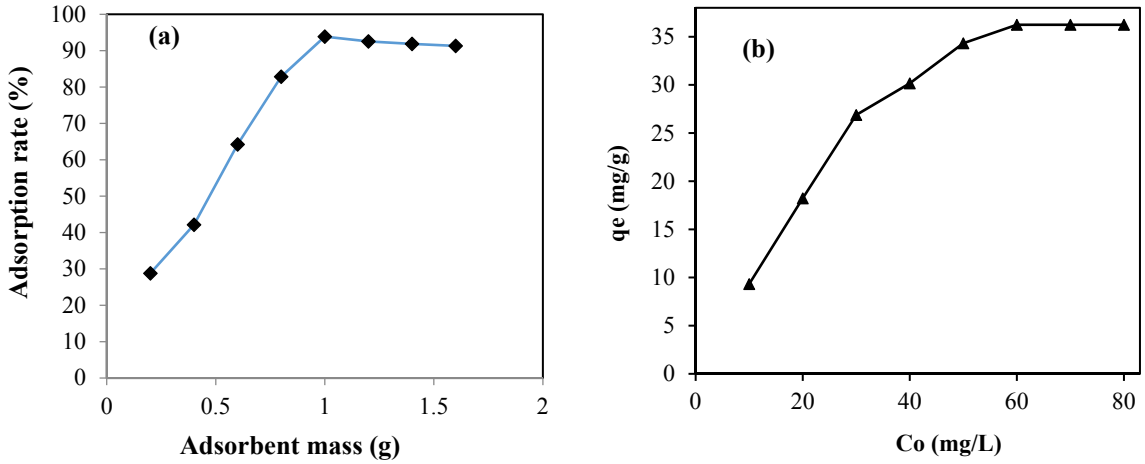

Fig. 4. a) Effect of adsorbent mass, b) Effect of initial concentration.

From equation 2, it has been noticed that the adsorption rate decreases with increasing initial Pb (II) concentration. This phenomenon can be explained by the inability of the surface of the solid at a constant number of sites to adsorb a quantity of ions in progression [37]. Moreover, it must be noted that a high initial concentration improves the diffusion of Pb (II) ions from the solution toward the adsorbent's active sites.

From the literature, it has been mentioned that the adsorption capacity of blast furnace slag is 53.58 mg of nickel per gram [22]. Blast furnace slag transformed into slag oxalate showed very good affinity for the adsorption of cobalt, where its maximum adsorption capacity is 576 mg/g [38]. Basic oxygen furnace slag showed good adsorption for a mixture of metal ions consisting of Cu, Cd, Pb, and Zn [39]. According to Table 2, BFS has a moderately acceptable adsorption capacity when compared to the adsorbents used in the processes for removing Pb (II) from solution.

3.3. Adsorption Isotherms

In the adsorption process, the interactions between adsorbent and adsorbable are generally identified by mathematical models. In this study, Freundlich, Langmuir and Temkin [47] isotherm models used to fit the equilibrium adsorption data. The linear form of the models of Freundlich, Langmuir and Temkin are presented respectively by equations 3-6.

$$\log q_e = \log k + \frac{1}{n}\log C_e \quad (3)$$

$$\frac{C_e}{q_e} = \frac{1}{q_{max}} C_e + \frac{1}{q_{max} b} \quad (4)$$

$$qe = B_T \ln A_T + B_T \ln Ce \quad (5)$$

$$B_T = \frac{RT}{b_T} \quad (6)$$

Where qe is the adsorbed amount (mg/g), Ce is the equilibrium concentration (mg L^{-1}); K_F represents the Freundlich constant, n is the characteristic constant associated with the temperature, q_{max} is the maximum capacity (mg/g) and b is the thermodynamic constant of the adsorption equilibrium ($L.mg^{-1}$), A_T is Temkin isotherm equilibrium binding constant (L/g), b_T is Temkin isotherm constant, R universal gas constant (8.314 J/mol/K) T is temperature at 298 K, and B_T is Constant related to heat of sorption (Kj $kmol^{-1}$).

Table 2. Comparison of uptake capacity of Pb(II) on various adsorbents

adsorbent	q_{max} (mg/g)	reference
Zeolite	14	[40]
Oak wood ash	47.16	[41]
Green tea	100	[42]
Mangosteen peel	130	[43]
Tobacco leaves	24.7	[44]
Activated carbon	22.8	[45]
Graphene oxide	36	[46]
BFS	34.26	This study

[DOI: 10.22068/ijmse.3011]

The parameters calculated from the models are represented in Table 3. The presentations of the models Freundlich, Langmuir, and Temkin are illustrated in Fig. 5. According to the results presented in table 3, the correlation coefficient of the Langmuir equation (R^2: 0.99) was higher than that of Freundlich (R^2: 083) and Temkin (R^2: 0.95). On the other hand, the maximum adsorption capacity calculated from the Langmuir model was closer to the measured value, which indicates that the Langmuir model is more appropriate for the Pb (II) adsorption on blast furnace slag in solution. This result allowed us to conclude that the Pb (II) adsorption in solution on the BFS was performed on a monolayer homogeneous surface.

The value of the Temkin model parameter (Bt) indicates that the interaction between Pb (II) ions and BFS in solution is physical [47], and the value of the Freundlich model's heterogeneity factor (n) indicates that adsorption is favorable [22] (Table 3).

The favorability of an adsorption process can be defined by the dimensionless separation factor (R_L). Indeed, the R_L will classify the isotherm as either favorable ($0 < R_L < 1$), unfavorable ($R_L > 1$), or linear ($R_L = 1$) [48].

$$R_L = \frac{1}{1+C_0 b} \quad (7)$$

Where R_L: the Ratio indicates the quality of the adsorption, b is the Langmuir isotherm constant and C_0 is the initial concentration.

Following the shape of the curve presented in Fig. 5(d), we have noticed the decrease in the value of the ratio R_L with the increase in the initial concentration and that this value was between 1 and 0, which allows us to conclude that the elimination of Pb (II) in solution on the BFS is favorable. Absolutely, this result confirms the previous hypothesis, where we mentioned the Freundlich parameter n ($1 < n < 10$) [49]. Importantly, the R_L values revealed that as initial concentration increased, adsorption efficiency decreased.

3.4. Adsorption Kinetics

Kinetic study of the Pb (II) adsorption automatically involves the use of our experimental data in very widespread and well-established models. In this study, we have used three adsorption kinetics models to evaluate the adsorption process in this case: pseudo first order, pseudo second order, and internal diffusion [33]. The models exploited are represented respectively by equations 8-10.

The Lagergren model shows that the occupancy ratio of the adsorption site is directly proportional to the unoccupied ratio, which indicates that the adsorbed substance only binds to a single active site on the surface of the adsorbent. And the adsorption process is physical adsorption.

$$\ln(q_e - q) = -k_{Lag} t + \ln(q_e) \quad (8)$$

$$\frac{t}{q} = \frac{1}{k_b q_e^2} + \frac{1}{q_e} \quad (9)$$

$$q = k_w \sqrt{t} + C \quad (10)$$

Where q_e is the adsorbed quantity at equilibrium (mg/g), q is adsorbed quantity at time t (mg/g), t is the time of adsorption process, k_{Lag} is the constant pseudo first order sorption speed (s^{-1}), k_b is the constant of pseudo second order sorption speed (min^{-1}), k_e is the coefficient of mass transfer through the outer film,, Co initial concentration (mg/L), C_e is the equilibrium concentration (mg/L), C_t is the concentration at time t (mg/L), k_w is the diffusion rate constant in the pores(mg/m. $min^{½}$) and C is the intercept and it's tied to the boundary layer.

The plot of ln (qe - qt) against time t was traced using the Lagergren equation Fig. 6(a) and the plot (t/qt) as a function t was traced using the Blanchard equation Fig. 6(b).

Based on the values in table 4, the pseudo second order model appears to be more appropriate for describing the Pb (II) adsorption process. In fact, the value of correlation coefficient $R^2_{Blanchard} > R^2_{Lagergren}$ and the values of calculated adsorption capacity and experimental adsorption capacity are close [22]. S.-Y. Liu et al. [50] discovered the same result.

Table 3. Isotherm parameters Pb(II) adsorption by BFS.

Freundlich	**K_F (mg.g^{-1})(ml.mg^{-1})$^{1/n}$**	**n**	**R^2**
	16.05	2.77	0.86
Langmuir	q_{max} (mg/g)	B (L.mg^{-1})	R^2
	38.46	2.77	0.99
Temkin	A_T (L/g)	B_T (KJ kmol^{-1})	R^2
	9.388	6.506	0.95

[DOI: 10.22068/ijmse.3011]

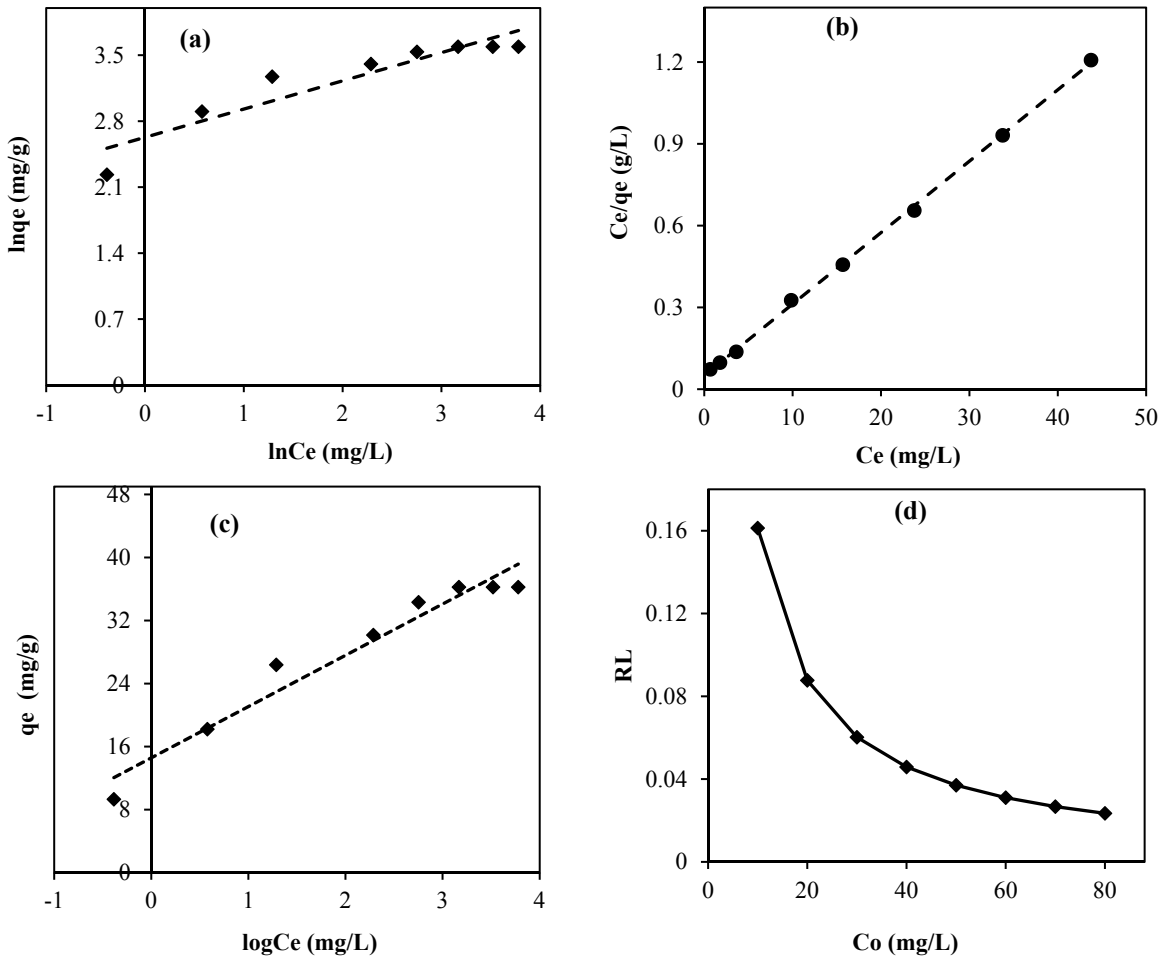

Fig. 5. a) Presentation of Freundlich model, b) Presentation of Langmuir model, c) Presentation of Temkin model, d) Evolution of RL ration as a function Co.

From Fig. 6, it was shown that the plot of adsorbed capacity (q) versus time (t) has no intercept (C= 3.86). Therefore, intraparticle diffusion is not the only mechanism that controls the adsorption process [51]. Indeed, Fig. 6(c) clearly depicts the various successive stages of Pb (II) diffusion from solution to adsorbent (BFS).
In the first step, the Pb (II) was transferred from solution to the external surface of the BFS through film diffusion. In the second step, the Pb (II) gradually diffused from the surface of the BFS towards the internal pores. This process stops at equilibrium. Consequently, we deduce that hat overall rate of Pb (II) adsorption in solution on BFS is controlled by two steps: the diffusion of the film on the outer surface and the intraparticle diffusion [52, 53].

3.5. Adsorption Thermodynamics

Thermodynamic parameters are very important, because shed precious insight into the nature of the ions metal adsorption process into solution. In this work, the variations in standard free energy (ΔG°), standard enthalpy (ΔH°) standard entropy (ΔS°) and the distribution coefficient were employed to study the feasibility and spontaneous nature of the Pb (II) adsorption on into solution by BFS. These thermodynamic parameters are studied by involving the equations 11, 12 and 13 [54].

$$\Delta G^0 = -RT\ln k_d \quad (11)$$

$$\ln k_d = \frac{\Delta H^0}{R} \times \frac{1}{T} + \frac{\Delta S^0}{R} \quad (12)$$

$$k_d = \frac{C_i - C_e}{C_e} \times \frac{V}{M} = \frac{q_e}{C_e} \quad (13)$$

By applying the function $\ln(k_d) = f(\frac{1}{T})$, we found the straight line presented in Fig. 6(d). The regression analysis has indicated a good correlation (R^2= 0.99). The slope (1.111 × 1000) represents $\frac{\Delta H}{R}$ and 3.369 corresponds at the intersection $\frac{\Delta S}{R}$.

[DOI: 10.22068/ijmse.3011]

Using equations 9, 10 and 11 we determined the thermodynamic parameters (Table 4).

From Table 4, it was observed that the values of the thermodynamic parameters, namely the free enthalpy variation (ΔG), enthalpy variation (ΔH) and entropy variation (ΔS) are negative.

The negative values of ΔG indicate that the Pb (II) adsorption by BFS is spontaneous and feasible [26]. The decrease in the value ΔG with increasing temperature reflects the adsorbent's high affinity for Pb (II) at 20°C. The negative value of ΔH indicates that the adsorption process is exothermic [55] and the low enthalpy value indicates that the adsorption process is physical (2 < ΔH< 21 kj/mole) [25]. The fact that ΔS value is negative indicates that during Pb (II) adsorption, the disorder at the solid/liquid boundary decreased [56].

The values of the free enthalpy (ΔG < 20kj/mole) show that the electrostatic interaction considerably influences the adsorption process of Pb (II) on the BFS [55].

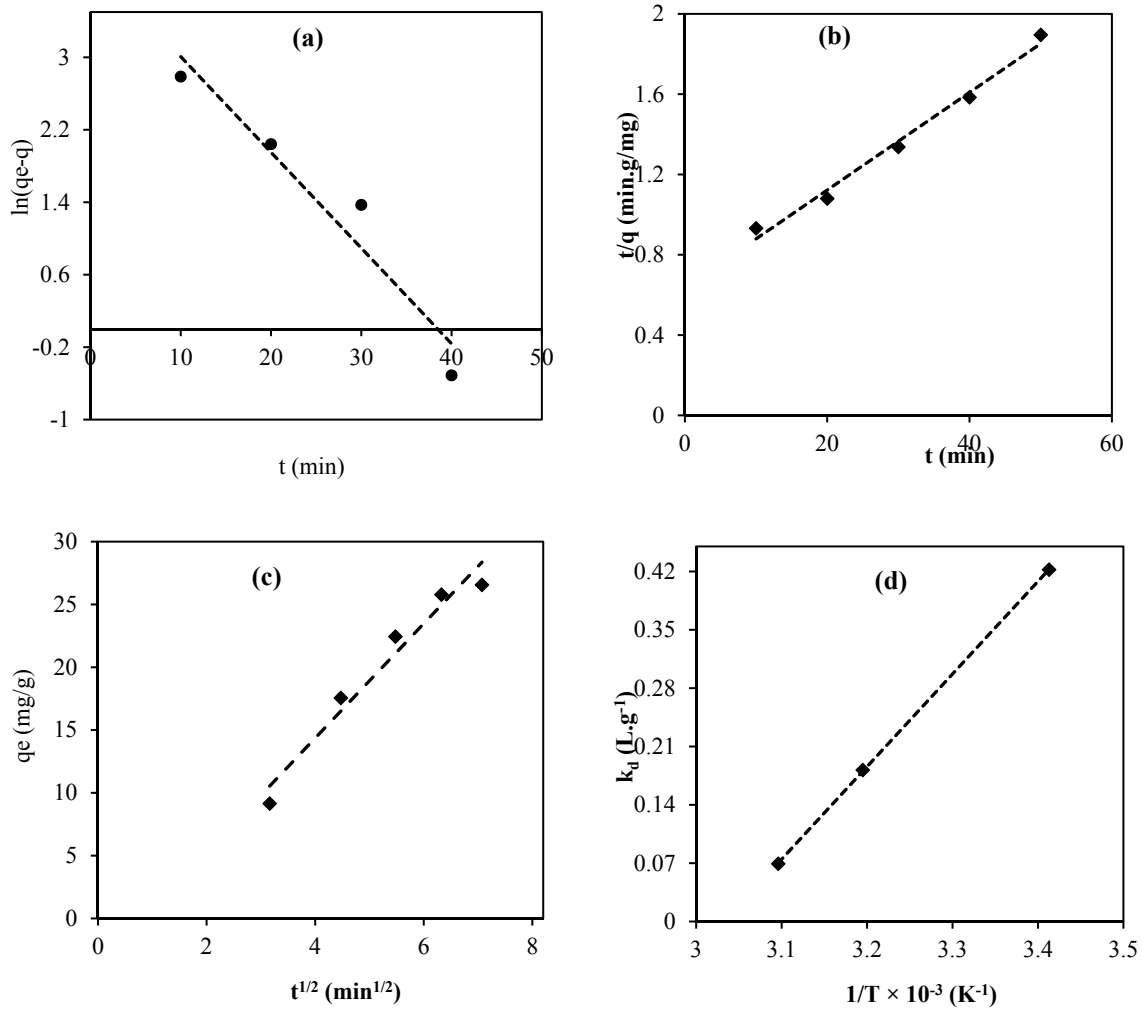

Fig. 6. Adsorption kinetics and thermodynamics: a) Pseudo first order kinetic, b) Pseudo second order kinetic, c) Internal diffusion kinetic, d) Van't Hoff plot for nickel adsorption by BFS.

Table 4. Kinetic parameters of Pb(II) adsorption on BFS

Lagergren model	K_{lag} (min^{-1})	qe_{theo} (mg/g)	R^2
	0.105	58.14	0.93
Blanchard model	K_b (g/mg min)	qe_{theo} (mg/g)	R^2
	9.05×10^{-3}	41.66	0.98
Internal diffusion	C (mg/g)	k_w ($mg/g.min^{0.5}$)	R^2
	3.86	4.55	0.95

[DOI: 10.22068/ijmse.3011]

Table 5. Thermodynamic parameters of the Pb(II) adsorption by BFS.

Temperature (K)	ΔH (kj/mole)	ΔG (kj/mole)	ΔS (j/mole.K)	K_d (L/g)
293	-9.23	-17.86	-28.25	1.525
313		-18.46		1.199
323		-18.75		1.071

4. CONCLUSIONS

In this research work, the Pb (II) adsorption on blast furnace slag (BFS) from aqueous medium was investigated as a function of contact time, initial pH, temperature, particle size and initial concentration. The physico-chemical characterization showed that the adsorbent consists mainly of the silica, lime, and alumina. The specific surface area of the BFS grains was around 275.8 m^2/g. The zero point of charge (ZPC) corresponded to a pH of 3.8. The equilibrium time was reached after 50 minutes of agitation. Pb (II) adsorption capacity was 36.24 mg/g with an 87.93% yield under ideal experimental conditions ($C_{0.}$: 60mg/L; V_{ag}: 150 rpm; pH: 5.4; Øs: 300 µm, T: 20°C; Ms: 1 g). The adsorption capacity declined with increasing temperature, indicating that lead adsorption is better at low temperatures (20°C). Modeling of the experimental data revealed that the Langmuir model was better suited to describe the isothermal behavior than the Freundlich and Temkin models. Which demonstrates that the lead removal process took place on a homogeneous monolayer surface. The kinetic studies revealed that the Pb (II) adsorption process was well fitted by pseudo-second order, with an R^2= 0.98 correlation coefficient. The mechanism of the transfer of Pb (II) ions from solution to BFS surface was studied, and it was discovered that the overall rate of adsorption was controlled successively by external diffusion and intarparticle diffusion. The thermodynamic study revealed that the elimination of Pb (II) on the BFS is spontaneous, exothermic, less entropic, and physical in nature, and the adsorption of Pb (II) is done by the electrostatic interaction. Finally, BFS can be used as a reliable and efficient adsorbent for Pb (II) elimination removal from waste water.

REFERENCES

[1] Wang, Z, Liu, J., Yang, Y., Yu, Y., Yan, X. and Zhang, Z., "AMn_2O_4 (A= Cu, Ni and Zn) sorbents coupling high adsorption and regeneration performance for elemental mercury removal from syngas", J. Hazard. Mater., 2020, 388, 121738.

[2] Awual, MR, "Mesoporous composite material for efficient Pb(II)(II) detection and removal from aqueous media". J. Environ. Chem. Eng., 2019a, 7, 103124.

[3] Shahat, A, Hassan, H.M.A., Azzazy, H.M.E., El-Sharkawy, E.A., Abdou, H.M. and Awual, M.R., "Novel hierarchical composite adsorbent for selective Pb(II)(II) ions capturing from wastewater samples", Chem. Eng. J., 2018, 332, 377-386.

[4] Verma, B, and Balomajumder, C., "Hexavalent chromium reduction from real electroplating wastewater by chemical precipitation". Bull. Chem. Soc. Ethiop., 2020, 34, 67-74.

[5] Abdullah, N, Yusof, N., Lau, W.J., Jaafar, J. and Ismail, A.F., "Recent trends of heavy metal removal from water/wastewater by membrane technologies", J. Ind. Eng. Chem., 2019, 76, 17-38.

[6] Bolisetty, S, Peydayesh, M. and Mezzenga, R., "Sustainable technologies for water purification from heavy metals: review and analysis", Chem. Soc. Rev., 2019, 48, 463-487.

[7] Barakat, MA, "New trends in removing heavy metals from industrial wastewater". Arabian J. Chem., 2011, 4, 361-377.

[8] Bashir, A, Ahmad, L., Sozia, M., Taniya, A., Mudasir, M. and Bhat, A.,"Removal of heavy metal ions from aqueous system by ion - exchange and biosorption methods. Environ", Chem. Lett., 2019, 17, 729-754.

[9] Chouchane, T, Yahi, M., Boukari, A., Balaska, A. and Chouchane, S., "Adsorption of the copper in solution by the kaolin", J. Mater. Environ. Sci., 2016, 7, 2825-2842.

[10] Tesfaw, B; Chekol, F.; Mehretie, S. and Admassie, S., "Adsorption of Pb(II) ions from aqueous solution using lignin from Hagenia abyssinica". Bull. Chem. Soc. Ethiop., 2016, 30, 473-484.

[11] Mohammed Alkherraz, A, Khalifa Ali, A.

[DOI: 10.22068/ijmse.3011]

and Muftah Elsherif, K., "Removal of Pb (II), Zn (II), Cu (II) and Cd (II) from aqueous solutions by adsorption onto olive branches activated carbon: equilibrium and thermodynamic studies". Chem. Int., 2020, 6, 11-20.

[12] Obayomi, K S and Auta, M., "Development of microporous activated Aloji clay for adsorption of Pb(II) (II) ions from aqueous solution", Heliyon, 2019, 5, e02799.

[13] Wang, H, Shang, H., Sun, X., Hou, L., Wen, M. and Qiao, Y.,"Preparation of thermo-sensitive surface ion-imprinted polymers based on multi-walled carbon nanotube composites for selective adsorption of Pb(II)(II) ion", Colloids Surf., A: Physicochem. Eng. Aspects, 2019, 585, 124139.

[14] Aigbe, R and Kavaz, D., "Unravel the potential of zinc oxide nanoparticle-carbonized sawdust matrix for removal of Pb(II) (II) ions from aqueous solution", Chinese J. Chem. Eng., 2021, 29, 92-102.

[15] Zare, EN, Lakouraj, M.M. and Masoumi, M., "Efficient removal of Pb (II) and Cd (II) from water by cross-linked poly (N-vinylpyrrolidone-co-maleic anhydride)@ eggshell/Fe_3O_4 environmentally friendly nano composite", Desalination Water Treat., 2018, 106, 209-219.

[16] Chen, W, Lu, Z., Xiao, B., Gu, P., Yao, W., Xing, J., Asiri, A.M., Alamry, K.A., Wang, X. and Wang, S., "Enhanced removal of Pb(II) ions from aqueous solution by iron oxide nanomaterials with cobalt and nickel doping", J. Clean. Prod., 2019, 211, 1250-1258.

[17] Wang, Y, Zuo, H. and Zhao, J., "Recent progress and development of ironmaking in China as of 2019: an overview", Iron Steel, 2020, 47, 640-649.

[18] Lei, Z, Jihao, C, Zhang, L., Huibin, H., Yusu, W and Yonghui, L., "Preparation of soybean oil factory sludge catalyst and its application in selective catalytic oxidation denitration process", J. Clean. Prod., 2019b, 225, 220-226.

[19] El-Dars, Farida M.S.E., Elngar, Marwa A.G., Abdel-Rahim, S.Th., El-Hussiny, N.A. and Shalabi, M.E.H. "Kinetic of nickel (II) removal from aqueous solution using different particle size of water-cooled blast furnace slag", Desalination Water Treat., 2015, 54, 769-778.

[20] Scott, I.S.P.C. and Penn, C.J., "Estimating the variability of steel slag properties and their influence in phosphorus removal ability", Chemosphere, 2021, 276, 130205.

[21] Dhmees, AS, Khaleel, N.M. and Mahmoud, S.A., "Synthesis of silica nanoparticles from blast furnace slag as cost-effective adsorbent for efficient azo-dye removal", Egypt. J. Petrol., 2018, 27, 1113-1121.

[22] Chouchane, T, Khireddine, O. and Boukari, A., "Kinetic studies of Ni(II) ions adsorption from aqueous solutions using the blast furnace slag (BF slag)", J. Eng. Appl. Sci., 2021, 68, 00039-3.

[23] Jiang, C, Wang, X., Hou, B., Hao, C., Li, X. and Wu, J., "Construction of a lignosulfonate-lysine hydrogel for the adsorption of heavy metal ions", J Agric Food Chem., 2020, 68, 3050-3060.

[24] Penido. ES, Melo. L.C.A., Guilherme. L.R.G. and Bianchi M.L., "Cadmium binding mechanisms and adsorption capacity by novel phosphorus/magnesium-engineered biochars", Sci. Total Environ., 2019, 671, 1134-1143.

[25] Droepenu, EK, Wee, B.S., Chin, S.F., Kok, K.Y. and Asare, E.A., "Adsorption of Zinc Oxide Nanoparticles onto Esterified Carbonize Sago Hampas: Kinetic and Equilibrium Studies", Iran. J. Mater. Sci., 2020, 17, 152-169.

[26] Iqbal, J, Wattoo, F.H., Wattoo, M.H.S., Malik, R., Tirmizi, S.A., Imran, M. and Ghangro, A.B., "Adsorption of acid yellow dye on flakes of chitosan prepared from fishery wastes", Arabian J. Chem. 2011, 4, 389-395.

[27] Wang, L, Fu, P., Ma, Y., Zhang, X., Zhang, Y. and Yang, X., "Steel slag as a cost-effective adsorbent for synergic removal of collectors, Cu(II) and Pb(II) ions from flotation wastewaters", Miner. Eng., 2022, 183, 107593.

[28] Baysal, Z, Cinar, E., Bulut, Y., Alkan, H. and Dogru, M., "Equilibrium and thermodynamic studies on biosorption of Pb (II) onto Candida albicans biomass", J. Hazard. Mater., 2009,161, 62-67.

[DOI: 10.22068/ijmse.3011]

[29] Bisiriyu, IO and Meijboom, R., "Adsorption of Cu(II) ions from aqueous solution using pyridine-2,6-dicarboxylic acid crosslinked chitosan as a green biopolymer adsorbent", Int. J. Biol. Macromol., 2020, 165, 2484-2493.
[30] Malik, A, Khan, A., Anwar, N. and Naeem, M., "A comparative study of the adsorption of congo red dye on rice husk, rice husk char and chemically modified rice husk char from aqueous media", Bull. Chem. Soc. Ethiop., 2020, 34, 41-54.
[31] Matsui, Y, Nakao, S., Sakamoto, A., Taniguchi, T. and Shirasaki, N., "Adsorption capacities of activated carbons for geosmin and 2-methylisoborneol vary with activated carbon particle size: Effects of adsorbent and adsorbate characteristics", Water Res., 2015, 85, 95-102.
[32] Chen, B, Sun, W., Wang, C. and Guo, X., "Size-dependent impact of inorganic nanoparticles on sulfamethoxazole adsorption by carbon nanotubes", Chem. Eng. J., 2017, 316, 160-170.
[33] Chouchane, T, Chouchane, S., Boukari, A. and Mesalhi, A., "Adsorption of binary mixture «Lead Nickel» by kaolin". J. Mater. Environ. Sci., 2015, 6, 924-941.
[34] Sabanovic, E, Memic, M., Sulejmanovic, J. and Selovic, A.," Simultaneous adsorption of heavy metals from water by novel lemon-peel based biomaterial", Pol. J. Chem. Technol., 2020, 22, 46-53.
[35] Malakahmad, A, Tan, S. and Yavari, S., "Valorization of wasted black tea as a low-cost adsorbent for Nickel and zinc removal from aqueous solution", J. Chem., 2016, 1, 1-8.
[36] Moshari, M, Mehrehjedy, A., Heidari-Golafzania, M., Rabbani, M. and Farhadi, S., "Adsorption study of Pb(II) ions onto sulfur/reduced graphene oxide composite", Chem. Data Coll., 2021, 31, 100627.
[37] Mustapha, S, Shuaib, D.T., Ndamitso, M.M., Etsuyankpa, M.B., Sumaila, A. and Mohammed, U.M., Nasirudeen, M.B., "Adsorption isotherm, kinetic and thermodynamic studies for the removal of Pb(II), Cd(II), Zn(II) and Cu(II) ions from aqueous solutions using Albizia lebbeck pods", Appl. Water Sci., 2019, 9, 142.
[38] Le, NQT, Vivas, E.L. and Cho, K., "Oxalated blast-furnace slag for the removal of Cobalt(II) ions from aqueous solutions". J. Ind. Eng. Chem. 2021, 95, 57-65.
[39] Xue, Y, Houa, H. and Zhu, S., "Competitive adsorption of copper(II), cadmium(II), lead(II) and zinc(II) onto basic oxygen furnace slag", J. Hazard. Mater., 2009, 162, 391-401.
[40] Rakhym, AB, Seilkhanova, G.A. and Kurmanbayev, T.S., "Adsorption of lead (II) ions from water solutions with natural zeolite and chamotte clay", Mater. Today: Proc., 2020, 31, 482-485.
[41] Pelalak, R, Heidari Z., Khatami, S.M., Kurniawan, T.A., Marjani, A. and Shirazian, S., "Oak wood ash/GO/Fe3O4 adsorption efficiencies for cadmium and lead removal from aqueous solution: Kinetics, equilibrium and thermodynamic evaluation", Arab. J. Chem., 2021, 14, 102991.
[42] Gameli, BHR, Duwiejuah, A.B. and Bawa, A.-A., "Adsorption of toxic metals from greywater using low-cost spent green tea as a novel adsorbent", Scientific African, 2022, 17, e01296.
[43] Kongsune, P., Rattanapan, S. and Chanajaree, R., "The removal of Pb^{2+} from aqueous solution using mangosteen peel activated carbon: Isotherm, kinetic, thermodynamic and binding energy calculation", Groundw. Sustain. Dev., 2021, 12, 100524.
[44] Yogeshwaran, V and Priya, A.K., "Adsorption of lead ion concentration from the aqueous solution using tobacco leaves", Mater. Today: Proc., 2021, 37, 489-496.
[45] Kobya, M, Demirbas, E., Senturk, E. and Ince, M., "Adsorption of heavy metal ions from aqueous solutions by activated carbon prepared from apricot stone", Bioresour. Technol. 2005, 96, 1518-1521.
[46] Lee, Y-C and Yang, J.-W., "Self-assembled flower-like TiO_2 on exfoliated graphite oxide for heavy metal removal", J. Ind. Eng. Chem., 2012, 18, 1178-1185.
[47] Chouchane, T and Boukari, A., "Impact of Influencing Parameters on the Adsorption of Nickel by Kaolin in an Aqueous Medium", Anal. Bioanal. Chem. Res., 2022, 9, 381-399.

[DOI: 10.22068/ijmse.3011]

[48] Venkata Ratnam, M, Vangalapati, M., Nagamalleswara Rao, K., and Ramesh Chandra, K., "Efficient removal of methyl orange using magnesium oxide nanoparticles loaded onto activated carbon", Bull. Chem. Soc. Ethiop., 2022, 36(3), 531-544.

[49] Bensalah, H, Younssi, S.A., Ouammou, M., Gurlo, A. and Bekheet, M.F., "Azo dye adsorption on an industrial waste-transformed hydroxyapatite adsorbent: Kinetics, isotherms, mechanism and regeneration studies", J. Environ. Chem. Eng., 2020, 3, 103807.

[50] Liu, S-Y, Gao, J., Yang, Y.-J., Yang, Y.-C. and Ye, Z.-X., "Adsorption intrinsic kinetics and isotherms of lead ions on steel slag", J. Hazard. Mater., 2010, 173, 558-562

[51] Demiral, H and Güng, C., "Adsorption of copper(II) from aqueous solutions on activated carbon prepared from grape bagasse", J. Clean., 2016, 124, 103-113.

[52] Lin, J and Zhan, Y., "Adsorption of humic acid from aqueous solution onto un-modified and surfactant-modified chitosan/zeolite composites", Chem. Eng. J., 2012, 200, 202-213.

[53] Liu, X and Zhang, L., "Removal of phosphate anions using the modified chitosan beads: Adsorption kinetic, isotherm and mechanism studies", Powder Technol., 2015, 277, 112-119.

[54] Ahmadi, A, Foroutan, R., Esmaeili, H. and Tamjidi, S., "The role of bentonite clay and bentonite clay@ $MnFe_2O_4$ composite and their physico-chemical properties on the removal of Cr (III) and Cr (VI) from aqueous media", Environ. Sci. Pollu. Res. Int., 2020, 14044-14057.

[55] Sarı, A, Cıtak, D. and Tuzen, M., "Equilibrium, thermodynamic and kinetic studies on adsorption of Sb(III) from aqueous solution using low-cost natural diatomite", Chem. Eng. J., 2010, 162, 521-527.

[56] Lei, T, Li, S.-J., Jiang, F., Ren, Z.-X., Wang, L.-L., Yang, X.-J., Tang, L.-H. and Wang, S.-X., "Adsorption of cadmium ions from an aqueous solution on a highly stable dopamine-modified magnetic nano-adsorbent", Nanoscale Res. Lett., 2019, 14. 152.

[DOI: 10.22068/ijmse.3011]